Asian Journal of Chemistry; Vol. 37, No. 4 (2025), 779-788

ASIAN JOURNAL OF CHEMISTRY

https://doi.org/10.14233/ajchem.2025.33337

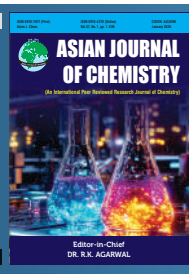

Investigations on the Synergistic Effects of Ionic Surfactants on Atenolol using Ultrasonics, Molecular Docking and ADMET Techniques

ADITYA GUPTA, INDU SAXENA*, SYED MOHAMMED EJAZ, DIVYANSHI MISHRA and PREETI YADAV

Department of Chemistry, University of Lucknow, Lucknow-226007, India

*Corresponding author: E-mail: indu_lu@yahoo.com

Received: 8 January 2025; *Accepted*: 19 February 2025; *Published online*: 29 March 2025; AJC-21937

Among the various ailments, cardiovascular diseases are particularly notable, requiring complex medication procedures that frequently come with unwanted side effects. β-Blockers cardiovascular drugs are in high usage due to cardiovascular diseases. Therefore, the present investigation explores an encouraging approach to improve the solubilization, drug delivery and excretion characteristics of the β-blocker drugs atenolol through a strategy derived from surfactants. The investigation focuses on the interaction between sodium dodecyl sulphate (SDS) and cetyltrimethylammonium bromide (CTAB) with atenolol. Employing a multifaceted approach, both physical and acoustic parameters across various solutions were explored. The relative density, viscosity, ultrasonic velocity of sound and specific conductance were determined as physical parameters. Physical findings reveal the increase in critical micelle concentration (CMC) value of SDS from 8.0-13.9 mmol. This synergistic molecular interactions between SDS and atenolol as depicted from physical, acoustical and computational (molecular docking and ADMET) analysis. Moreover, the enhanced solubilization of atenolol in the presence of SDS as supported by CMC values, underscores the potential of surfactant in drug delivery and excretion applications. Furthermore, the acoustic parameters such as adiabatic compressibility, acoustic impedance, viscous relaxation time and intermolecular free length support the findings.

Keywords: Cardiovascular drugs, Ionic surfactants, Acoustic parameters, Drug delivery, Molecular docking, ADMET analysis.

INTRODUCTION

In today's world, a plethora of diseases afflict people, causing both biological disturbances and mental stress [1]. These ailments, often stemming from sedentary lifestyles and poor dietary habits, have become increasingly prevalent even among younger individuals [2]. The cardiovascular diseases including heart failure have seen a concerning rise among young adults in recent years, underscoring the importance of prevention and early intervention [3]. Surfactants, organic compounds featuring both hydrophilic and hydrophobic components within a single molecule, exhibit amphiphilic properties and form micelles in aqueous solutions [4-6]. The primary characteristic of their aggregation phenomena originates from a range of noncovalent interactions performing at the molecular scale [7-9]. These molecules play a crucial role in various applications, including biotechnology and disinfection [10-16]. Sodium dodecyl sulfate, a well-studied anionic surfactant, finds utility across diverse fields such as polymer biotechnology and pharmaceuticals [17,18]. Cetyltrimethylammonium bromide (CTAB), a cationic surfactant and like surfactants gained an upsurge in demand after a pandemic for analogues [19-21].

Cardiovascular drugs, including atenolol, a β-blocker, are vital for managing heart-related conditions such as hypertension and angina [22]. It works by blocking β-1 adrenergic receptors in the heart, thus decreasing the heart rate and workload. However, like other drugs, atenolol comes with potential side effects, emphasizing the importance of careful management and monitoring [13,23]. Solubility stands as a vital parameter for achieving therapeutic drug concentrations in the bloodstream. The solubility or dissolution rate of a drug is key in determining its absorption rate and extent, significantly impacting its bioavailability. Poor water solubility, particularly in lipophilic drugs for oral absorption (BCS Class II), poses a significant challenge for formulation developers. Various approaches, such as micronization, chemical alteration, pH adjustment, solid dispersion, complexation, co-solvency and surfactant utilization, aim to enhance solubility [24]. Low aqueous solubility presents a pri-

mary hurdle in the formulation development of New Chemical Entities (NCEs) and generics. Enhanced solubility is especially desired in formulations like mouth-dissolving tablets and solid dispersions for faster onset of action [25].

Previous study shows that the surfactants have gained attention for solubility enhancement due to their ease of use, effectiveness in small concentrations, compatibility with a wide range of drugs and minimal issues in animal and human subjects [26-30]. This study focuses on the elucidation of the interactions between the β-blocker drug atenolol with different surfactants. The present research specifically aims to investigate the interaction between ionic surfactant and atenolol in an aqueous micellar system. We utilize various physical and acoustic parameters to evaluate the outcomes of these interactions. Moreover, the molecular docking analysis between surfactant and drug molecule provides further insight into these interactions. The results obtained from molecular docking analysis are compared with those achieved in aqueous anionic, cationic and anionic-cationic micellar systems. Through this comprehensive approach, the understanding of drug-surfactant interactions can be explored, which can help to develop more effective pharmaceutical formulations and treatments.

EXPERIMENTAL

The experiment was conducted in an aqueous medium prepared meticulously using tap water subjected to a rigorous purification process. Initially, standard tap water, containing chlorine and with a conductivity ranging from 2-5 × 10^{-6} S cm^{-1} at 298 K, underwent distillation using a millipore distillation unit. The purified water exhibited conductivities of approximately 1-4 × 10^{-7} S cm^{-1} at 298 K. The highly purified water was utilized throughout the experimental procedures.

The surfactants employed in this study were sodium dodecyl sulphate (SDS, Fisher Scientific, LR grade; purity > 99%, CAS No. 151-21-3) and cetyltrimethylammonium bromide (CTAB, S.D. Fine Chemicals Ltd., LR grade; purity > 99%, CAS No. 57-09-0). To ensure the accuracy and reliability of the results, both surfactants were purified through recrystallization using ethanol. Atenolol, a β-blocker drug marketed under the brand name ATEN™-100 by Zydus Cadila, was used after the extraction of the active drug part from tablets.

Extraction of drug: The active part of drug was obtained after the removal of excipients using dissolution and filtration with methanol [31,32].

Characterization: FTIR spectra were recorded using Shimadzu FT-IR analyzer in the wavelength range of 4000-500 cm^{-1}. The UV spectra were recorded using a UV analyzer operating within the range of 200-1100 nm in the aqueous medium. The ^{1}H and ^{13}C NMR spectra were recorded using Bruker Avance-300 instrument. The samples were prepared in DMSO-d_6. The spectra were recorded solely for the extracted part to determine the purity of the extracted part of drug. The spectra were obtained simply for the isolated component to assess the purity of the extracted drug portion. For better study of interactions, other NMR spectra were also recorded to determine the effect of the addition of surfactant with the atenolol. For this mixed surfactant-atenolol solution was prepared in DMSO-d_6 solvent.

Determination of critical micelle concentration: A graph showing the relationship between the specific conductance (K) was measured with a digital conductivity meter (STI 475, Sky Technology, India) with an accuracy of about ±0.2% and the molar concentration (m) of surfactant solution. The CMC was subsequently calculated at the intersection point [33].

Molecular docking: The optimized structures of all the molecules were obtained by employing the B3LYP/6–31 G method and the Gaussian16 software program [34], without imposing any topological constraints, while adhering to the stringent convergence criteria. AutoDock 4.2.6 software was used to explore the interaction between the ionic surfactant (receptors; SDS as an anionic receptor and CTAB as a cationic receptor) and the atenolol molecule (ligand) in an aqueous medium.

ADMET analysis: The characterized molecule was designed using the MarvinSketch® software of the ChemAxon© software package Marvin JS. These properties are used as molecular descriptors for pharmacokinetic properties. They are used in the theoretical calculation of the physicochemical properties of ionization (pK_a), partition coefficient (log P), distribution coefficient (log D), water solubility (log S) and polarity (PSA). Then, for establishing the pharmacokinetic features of the ADME models, the SMILES of each molecule were uploaded to the SwissADME web servers. Furthermore, drug similarity and pharmacokinetic predictions were applied to bioavailability scores and Lipinski, Ghose and Veber rules. The toxicity of the compounds was evaluated using web server PRO TOX II, which gave the predicted values after theoretical calculations.

Thermophysical and acoustic parameters determination

Preparation of mixed ionic surfactant solution: For further interactive studies, several solutions were prepared to explore the interaction between SDS and CTAB in the absence and presence of atenolol. These prepared solutions were employed to elucidate the complexities of molecular interactions. Nine distinct clear solutions containing varying mole fractions of SDS and CTAB were prepared in fixed ratios as outlined in Table-1.

Thermophysical parameters: The thermophysical parameters like relative density (ρ_r), relative viscosity (V_r) and ultrasonic velocity of sound (u) were evaluated using eqns. 1-3:

Relative density (ρ_r) measurements were conducted by the magnetic float densimeter [35] kept in a constant heat reservoir using eqn. 1:

TABLE-1
THE MOLE FRACTION OF RESPECTIVE SOLUTIONS

Solution	Solution ratio								
	A	B	C	D	E	F	G	H	I
SDS:CTAB	01:00	0.9:0.1	0.88:12	0.86:0.14	0.84:0.16	0.82:0.18	0.8:0.2	0.78:0.22	0.76:0.24

$$\text{Relative density } (\rho_r) = \frac{(W + w + f.I)}{\left(V + \frac{w}{d_{pt}}\right)} \quad (1)$$

where w = weight used, I = current passed through the circuit, d_{pt} = weight of platinum (W) and V = volume of the float.

The relative viscosity (V_r) of the different solutions was determined utilizing an electro-viscometer. Remarkably, the precision achieved in these measurements was approximately ± 0.02% and calculated using eqn. 2:

$$\frac{V_r}{V_w} = \frac{\rho_s}{\rho_w} \times \frac{t_s}{t_w} \quad (2)$$

The equation involves terms representing viscosity (V_w), density (ρ_w) and flow time (t_w) of water, alongside viscosity (V_r), density (ρ_s) and flow time (t_s) of the unknown liquid mixture.

The ultrasonic velocity of sound (u) was determined using a high-precision multi-frequency ultrasonic interferometer. It was determined using eqn. 3:

$$\text{Ultrasonic velocisty } (u) = \lambda \times f \quad (3)$$

where λ is the path difference and f is the applied frequency.

Acoustic parameters: The acoustic parameters function as essential indicators, providing detailed insights into the behavior of molecular interactions within these systems. These parameters were determined using eqns. 4-7:

Adiabatic compressibility (β_{ad}) was elucidated using eqn. 4:

$$\beta_{ad} = \frac{1}{\rho_r . u^2} \quad (4)$$

here ρ_r is the relative density and u is the ultrasonic velocity of the respective solution.

The acoustic impedance (Z) was elucidated using eqn. 5:

$$z = \rho_r \times u \quad (5)$$

here ρ_r is the relative density and u is the ultrasonic velocity of the respective solution.

The intermolecular free length (L_f) was elucidated using eqn. 6:

$$L_f = K_T . \beta_{ad}^2 \quad (6)$$

here, K_T is the free length constant, which had been calculated using a formula, $K_T = (93.875 + 0.345T) \times 10^{-8}$, here, T is the temperature at which the experiment was performed.

At 298 K and 308 K, the values were found to be 196.685 × 10^{-8} K and 200.135 × 10^{-8} K, respectively.

The viscous relaxation time (τ) was elucidated using eqn. 7:

$$\tau = \frac{(4 V_r \beta_{ad})}{3} \quad (7)$$

here, V_r is relative viscosity and β_{ad} is adiabatic compressibility.

RESULTS AND DISCUSSION

Extraction of drug: The analyzed extract of drug was determined to be pure and free of excipients, as compared to the reference spectral FTIR, UV and NMR spectral data reported in the literature [36]. The isolated pure component of the drug was utilized in all formulations.

CMC analysis: The micellization behaviour of sodium dodecyl sulfate (SDS) and cetyltrimethylammonium bromide (CTAB) was closely examined in the context of drug-surfactant interactions. Plots depicting the dependence of specific conductance (κ) on the molar concentration (m) of these surfactants solely and in aqueous atenolol-surfactant solution revealed using the breakpoint. The breakpoint is observed in Fig. 1, which gives the respective CMC value. The CMC values of the respective surfactant solution are shown in Table-2.

TABLE-2
THE VALUES OF CMC FOR BOTH SURFACTANT SOLUTION

Solutions	CMC value × 10^{-3} molar			
	CTAB		SDS	
	298 K	308 K	298 K	308 K
1.5 mM drug	0.978	0.994	10.876	11.127
7.5 mM drug	1.031	1.093	13.547	13.932

The critical micelle concentration (CMC) values of CTAB, a positively charged surfactant, were found to fall within the range of 0.95 to 1.1 mmol L^{-1}, which closely aligns with the CMC of CTAB in pure aqueous solution (0.85 mmol L^{-1}) [25]. This consistency suggests that the presence of atenolol does not significantly alter the micellization behaviour of CTAB. In contrast, a significant difference was observed with SDS, a negatively charged surfactant exhibiting a CMC of 8 mmol L^{-1} in water. In presence of drug atenolol, SDS exhibited substantially increased CMC values, ranging from 1.5 to 7.5 mmol L^{-1}. This disparity indicates a distinct interaction between SDS and atenolol, impacting the micellization behaviour of SDS. Literature suggests that the largest solubilities of the cardiovascular β-blocker drug are observed in aqueous micellar solutions of anionic surfactants. This phenomenon is attributed to the formation and solubilization of ion pairs of the cationic form of the drug with surfactant anions [37]. Furthermore, the extent of solubilization of atenolol varies significantly depending on the type of surfactant molecule present. Specifically, the order of solubilization efficacy is:

Anionic surfactant > Cationic surfactant

This order signifies that anionic surfactants have a more significant impact on drug solubilization than cationic surfactants. The delayed micellization observed in SDS solutions with atenolol demonstrates the substantial impact of anionic surfactants on the solubilization process.

NMR studies of mixed surfactant and atenolol: To obtain more insight through NMR spectral data, the active component of drug and anionic surfactant were mixed and then ^{1}H and ^{13}C spectra were recorded, which is shown in Fig. 2a-b. The presence of a broad and weak peak at 7.427 ppm suggests that the NH (35H) linkage (in drug) is not as robust as observed in the spectra of the extracted pure drug. This indicates that upon the addition of anionic surfactant to atenolol, the N-H linkage (29H and 35H) weakens (Fig. 2a). This weakening of the N-H bond (in drug) strongly implies the formation of hydrogen

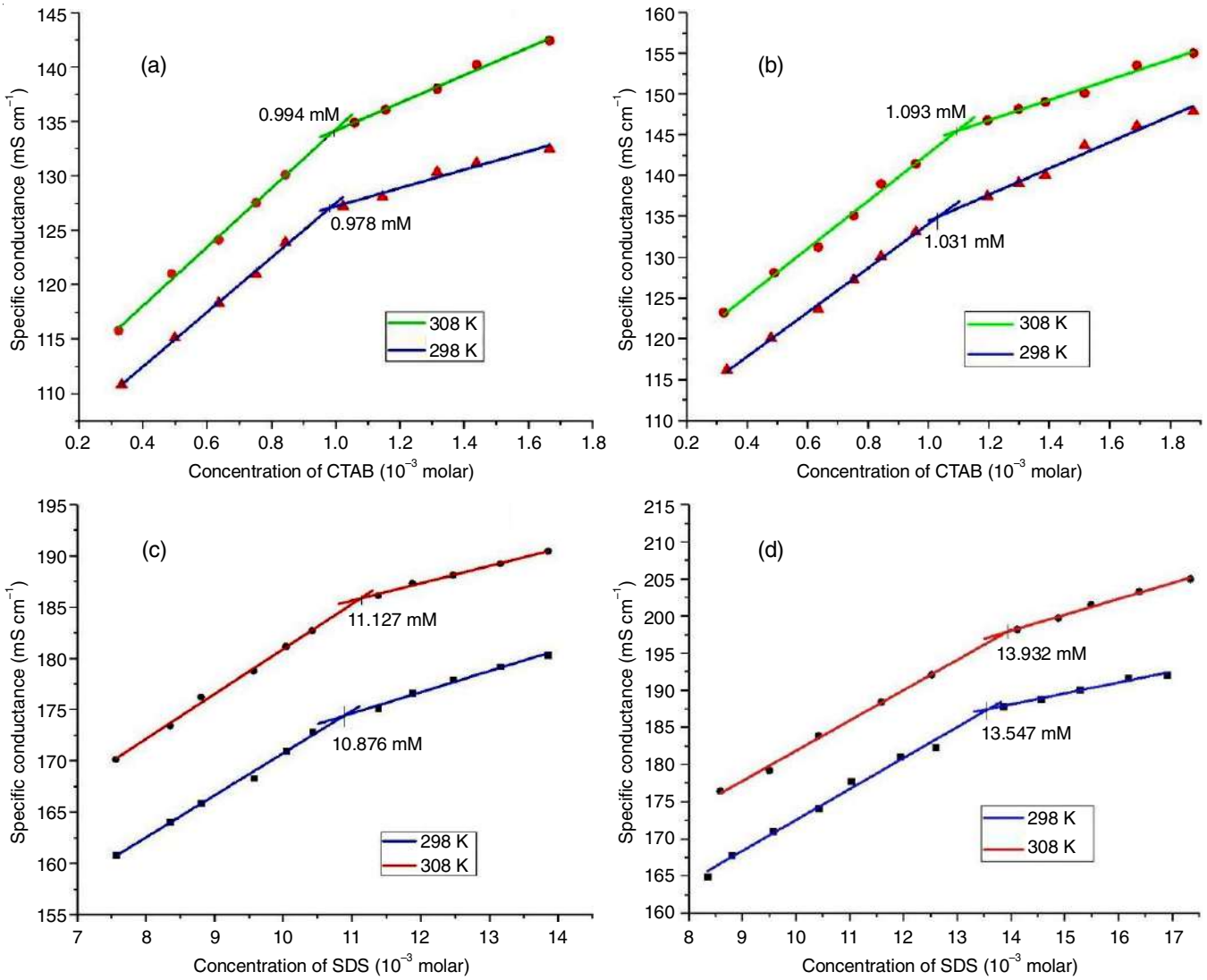

Fig. 1. The CMC values (a) of CTAB with 1.5 mM drug solution (b) of CTAB with 7.5 mM drug solution (c) of SDS with 1.5 mM drug solution (d) of SDS with 7.5 mM drug solution

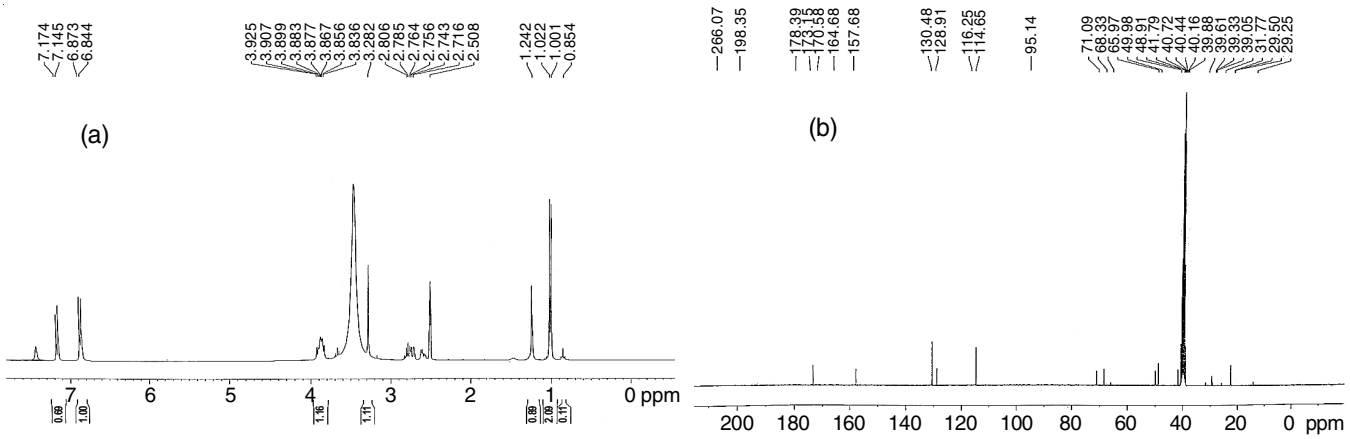

Fig. 2. (a) ^{1}H and (b) ^{13}C NMR spectra of a mixture containing SDS and the drug's extracted part

bonds between the N-H group of atenolol and the anionic component of the surfactant (O^- & O^-). This observation provides compelling evidence for the occurrence of hydrogen bonding interactions between atenolol and the anionic surfactant.

Molecular docking studies: Molecular docking studies unveiled compelling interactions between the anionic receptor (SDS) and the ligand (atenolol) molecule, characterized by the formation of hydrogen bonds. At the binding site, three

hydrogen bonds were observed between the anionic receptor (SDS) and the ligand (atenolol) molecules while there was no interaction between the ligand and cationic receptor molecule. Specifically, the O16 atom of the anionic receptor (-S=O linkage in anionic receptor) forms hydrogen bonds with the H32 atom (-OH linkage) O16···H32 (1.77 Å) and also with the H35 atom of the ligand (-NH linkage) O16···H35 (1.73 Å). Additionally, the O13 atom in the anionic receptor (C-O-S linkage of SDS) exhibited hydrogen bonding with the H29 atom of ligand (N-H of -$CONH_2$) O13···H29 (1.95 Å). These interactions underscore the strong affinity of the anionic receptor, SDS, for atenolol, as depicted in Fig. 3a-b and also corroborated in Tables 3 and 4. Conversely, the molecular docking analysis between the cationic receptor CTAB and the ligand revealed no discernible interaction, as illustrated in Fig. 3c.

The best-docked conformations are found using the clustering histogram with different RMSD values, which calculates the RMSD between the predicted conformation of AutoDock4 and the actual structure with low binding energy conformations. The conformations in each bin of the clustering histogram are within two RMSD of the optimal docking conformation.

TABLE-3
THE SUMMARY OF BINDING ENERGIES (kcal/mol) AND THE H-BOND INTERACTIONS: DETAILS OF THE MOLECULAR DOCKING DATA

Receptor	No. of H-bonds	Inhibition constant (mM)	Binding energy (ΔG) (kcal/mol)
Cationic (CTAB)	0	896.51	-0.06
Anionic (SDS)	3	22.12	-2.26

Compound clustering histograms are displayed in Fig. 4. The estimated binding energies for the complex are shown in Table-5.

ADMET analysis: The smile files of all the molecules (atenolol, SDS and the drug-SDS complex) were uploaded and elucidated its properties. The data obtained covers the computational elucidation of drug-likeness, solubilities, lipophilicity and toxicity behaviour of the components.

Drug likeness properties: Drug likeness properties of the molecules are shown in Table-6. The active drug must not violate more than one of the following properties: molecular weight (MW) ≤ 500, log P ≤ 5, hydrogen bond acceptors ≤ 10 and hydrogen bond donors ≤ 5 [38].

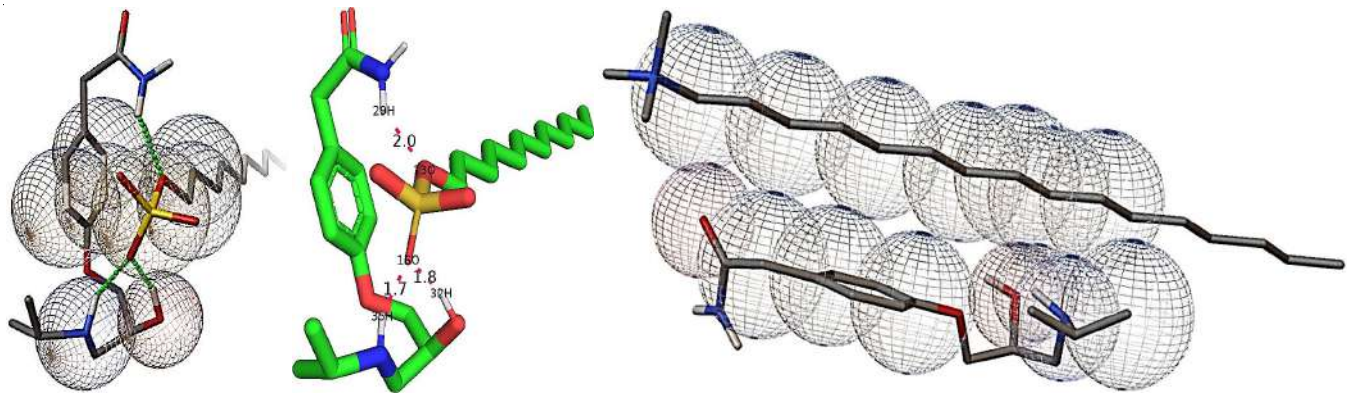

Fig. 3. (a) Interaction between active sites of anionic receptor and ligand, (b) Hydrogen bonds and their distance between anionic receptor and ligand and (c) Interaction between cationic receptor molecule and ligand

TABLE-4
CLUSTER ANALYSIS OF CONFIRMATIONS WITH BOTH RECEPTORS WITH RMSD VALUES AND BINDING ENERGIES WITH LIGAND (DRUG) MOLECULE

Anionic receptor (SDS)			Cationic receptor (CTAB)		
Cluster rank	Conformation score	Binding energy (kCal/mol)	Cluster rank	Conformation score	Binding energy (kCal/mol)
1	2	-2.26	1	40	-0.06
2	15	-2.14	2	16	-0.05
3	28	-2.13	3	2	-0.02
4	22	-2	4	17	0
5	12	-1.98	5	33	0.01

TABLE-5
ESTIMATED BINDING ENERGIES FOR BOTH RECEPTORS WITH A LIGAND MOLECULE

Molecule	Estimated free energy of binding (kcal/mol)	Final intermolecular energy (kcal/mol)	vdW + H-bond + desolv energy (kcal/mol)	Electrostatic energy (kcal/mol)	Final total internal energy (kcal/mol)	Torsional free energy (kcal/mol)	Unbound system's energy = (2) (kcal/mol)
Cationic receptor	-0.06	-2.75	-2.74	-0.01	-2.97	2.68	-2.97
Anionic receptor	-2.26	-4.94	-3.3	-1.64	-2.28	2.68	-2.28

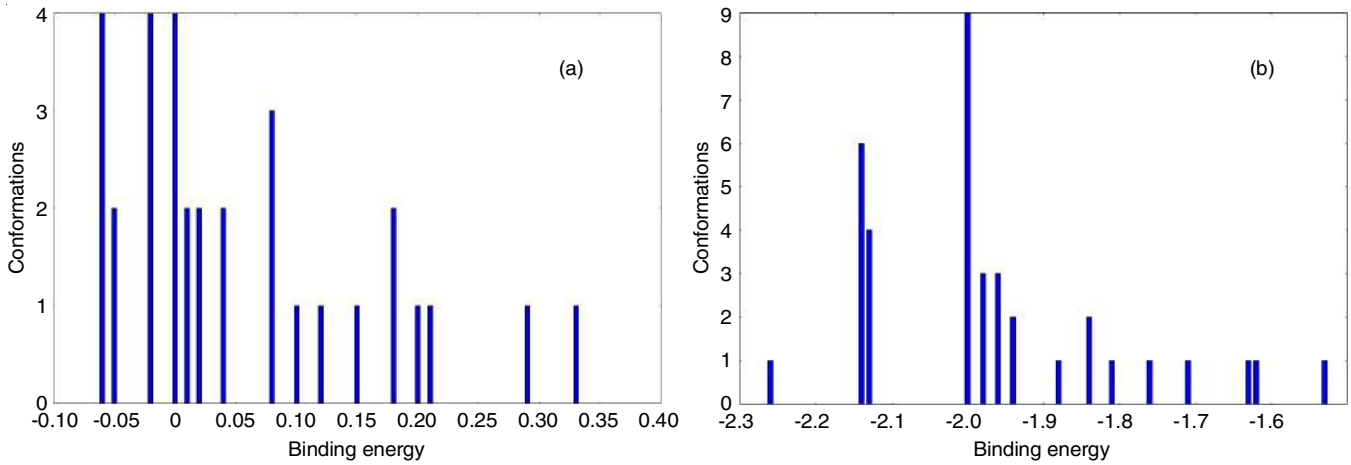

Fig. 4. Histograms of atenolol with (a) CTAB (cationic receptor) (b) SDS (anionic receptor) molecules with binding energies out of 40 runs using an RMSD-tolerance of 2.0 Å with different conformational clusters

TABLE-6
DRUG LIKENESS PROPERTIES OF THE COMPONENTS

Compound	Drug likeness			Bioavailability score
	Lipinski	Ghose	Veber	
Atenolol	Yes; 0 violation	Yes	Yes	0.55
SDS	Yes; 0 violation	Yes	No; 1 violation: Rotors > 10	0.85
Complex	Yes; 1 violation: MW > 500	No; 3 violations: MW > 480, MR > 130, #atoms > 70	No; 2 violations: Rotors > 10, TPSA > 140	0.55

The active drug must meet the following criteria: polar surface area (PSA), rotatable bonds (rotatable bonds <10) and total hydrogen bonds (≤ 12). The polar surface area of less than 140 has an oral bioavailability of at least 20% [39]. The active drug has Log P (– 0.4~5.6), molar refractivity (40~150), MW (160~480), number of atoms (20~70) and polar surface area (PSA) < 140, as per Ghose criteria [40]. Based on the drug-likeness analysis, all the compounds were found by the Lipinski's rule (Table-6). Furthermore, atenolol and SDS obeyed Ghose's rules and only atenolol complied with Veber's rule.

Solubility behaviour: The topological technique was used to determine solubility is called log S (ESOL) [41]. The enhancement of solubility of the complex in comparison to SDS is feasible as shown in Table-7. The order is found to be as follows:

Not soluble <-10 \poorly<-6~ moderately<-4 ~ soluble < -2< very 0< highly.

Lipophilicity properties: Based on the compound's ilog P value presented in Table-8, atenolol exhibits moderate hydrophilicity, suggesting a preference for dissolution in polar solvents rather than non-polar solvents. The molecule is very lipophilic, with a considerable tendency to dissolve in non-polar solvents as opposed to polar solvents, as indicated by the log P value of the SDS and complex.

TABLE-8
LIPOPHILICITY PROPERTIES OF THE COMPONENT

Compound	log $P_{O/W}$ (i log P)
Atenolol	0.480
SDS	3.563
Complex	3.510

Since atenolol is a well-known drug, so all of the parameter values on a radar chart fall inside the red area shown in Fig. 5a, which usually means that the compound's molecular properties are within acceptable bounds or thresholds for becoming a drug or having other desired attributes. The lipophilicity is relatively of SDS low because it falls beyond the red area. The compound has a higher polarity than the first compound since it is placed further from the center along the polar axis shown in Fig. 5b, which shows similar flexibility with the first one, as they both fall within the red zone.

The complex exhibits higher polarity than both surfactants, as it is positioned further from the center along the polar axis, illustrated in Fig. 5c, indicating that the complex possesses increased flexibility compared to both surfactants. Alterations in the molecular features may affect the pharmacokinetic behaviour of the complex and its applicability in drug research and development.

TABLE-7
SOLUBILITY BEHAVIOUR OF THE COMPONENTS

Compound	log S (ESOL)	Solubility	Class
Atenolol	-1.008	1.34×10^{1} mg/mL; 5.04×10^{-2} mol/L	Highly soluble
SDS	-3.955	5.55×10^{-2} mg/mL; 2.09×10^{-4} mol/L	Soluble
Complex	-3.144	1.36×10^{-1} mg/mL; 2.57×10^{-4} mol/L	Soluble

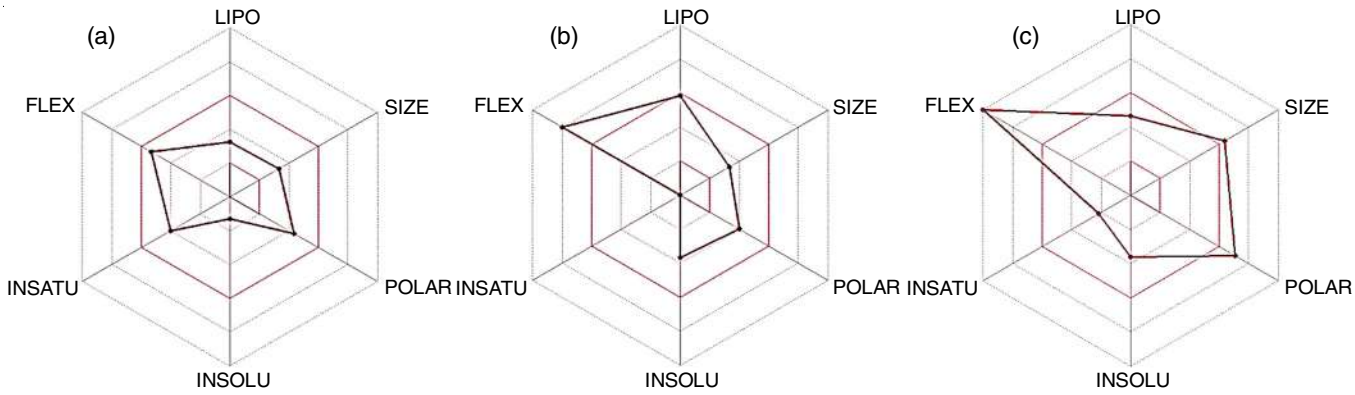

Fig. 5. Radar charts of (a) atenolol (b) SDS (c) complex

Toxicity: Toxicity data obtained from the ADMET analysis are shown in Fig. 6. The LD_{50} value is the dose of a drug that is deadly to 50% of the test population (usually measured in mg per kg of body weight). Usually, a higher LD_{50} number denotes lesser toxicity and implies that the substance is comparatively less harmful. The complex comes out to be non-toxic as it possess a very high LD_{50} value of 2000 mg/kg.

Experimental analysis of solution prepared

Thermophysical properties analysis: The properties outlined in eqns. 1-3 were empirically determined for the solutions and the corresponding results measured at distinct temperatures, at 298 K and 308 K and shown in Table-9.

Acoustic parameters analysis: Acoustic parameters were evaluated using eqns. 4-7 and the obtained values are shown in Table-10. The adiabatic compressibility indicates the proportional reduction in volume per unit rise in absolute pressure during a process that occurs without any heat transfer. It has been observed that there is a significant decrease in the adiabatic compressibility value as the mole fraction of CTAB increases, as well as with the addition of atenolol.

TABLE-9
VALUES OF RELATIVE DENSITY, RELATIVE VISCOSITY AND ULTRASONIC VELOCITY IN THE ABSENCE AND PRESENCE OF ATENOLOL

Mole fraction ratio of SDS:CTAB solution	Pure surfactant solution		Surfactant solution with 1.5 mM drug		Surfactant solution with 7.5 mM drug	
	298 K	308 K	298 K	308 K	298 K	308 K
Relative density (ρ) (Kg/m^3)						
A	998.957	998.193	999.372	998.865	999.762	999.025
B	1005.068	1002.962	1006.302	1004.017	1007.493	1005.263
C	1006.942	1004.235	1007.242	1004.914	1008.541	1006.017
D	1007.676	1004.981	1008.825	1005.312	1009.267	1006.592
E	1008.535	1005.624	1009.134	1006.137	1010.029	1007.537
F	1009.159	1006.728	1009.961	1007.093	1010.784	1008.669
G	1009.877	1008.179	1010.297	1008.454	1011.478	1010.028
H	1011.155	1009.514	1011.647	1009.815	1012.637	1011.134
I	1012.418	1010.167	1012.893	1010.562	1014.188	1012.076
Relative viscosity (V_r) (mPa sec)						
A	0.9538	0.9479	0.9612	0.9513	1.0131	0.9895
B	0.9581	0.9506	0.9679	0.9591	1.0431	1.0143
C	0.9613	0.9573	0.9704	0.9648	1.0858	1.0681
D	0.9652	0.9619	0.9793	0.9716	1.1072	1.0853
E	0.9694	0.9683	0.9835	0.9785	1.1359	1.1028
F	0.9796	0.9717	0.9903	0.9837	1.1765	1.1627
G	0.9849	0.9793	0.9987	0.9884	1.2031	1.1893
H	0.9978	0.9876	1.0125	0.9987	1.2516	1.2075
I	1.1012	1.0872	1.1205	1.1028	1.2743	1.2465
Ultrasonic velocity (U) (m/s)						
A	1504.468	1501.872	1505.019	1503.745	1509.546	1507.142
B	1506.746	1503.143	1507.175	1504.978	1510.145	1508.548
C	1508.125	1505.785	1508.885	1507.237	1512.621	1510.129
D	1509.891	1507.017	1510.073	1508.795	1513.924	1512.821
E	1511.273	1508.683	1512.285	1510.178	1515.689	1513.986
F	1513.634	1509.881	1514.059	1511.953	1518.135	1515.204
G	1514.582	1511.863	1515.981	1513.079	1520.274	1517.152
H	1517.230	1513.127	1518.862	1516.148	1523.784	1519.554
I	1519.769	1516.497	1522.543	1520.085	1527.857	1524.792

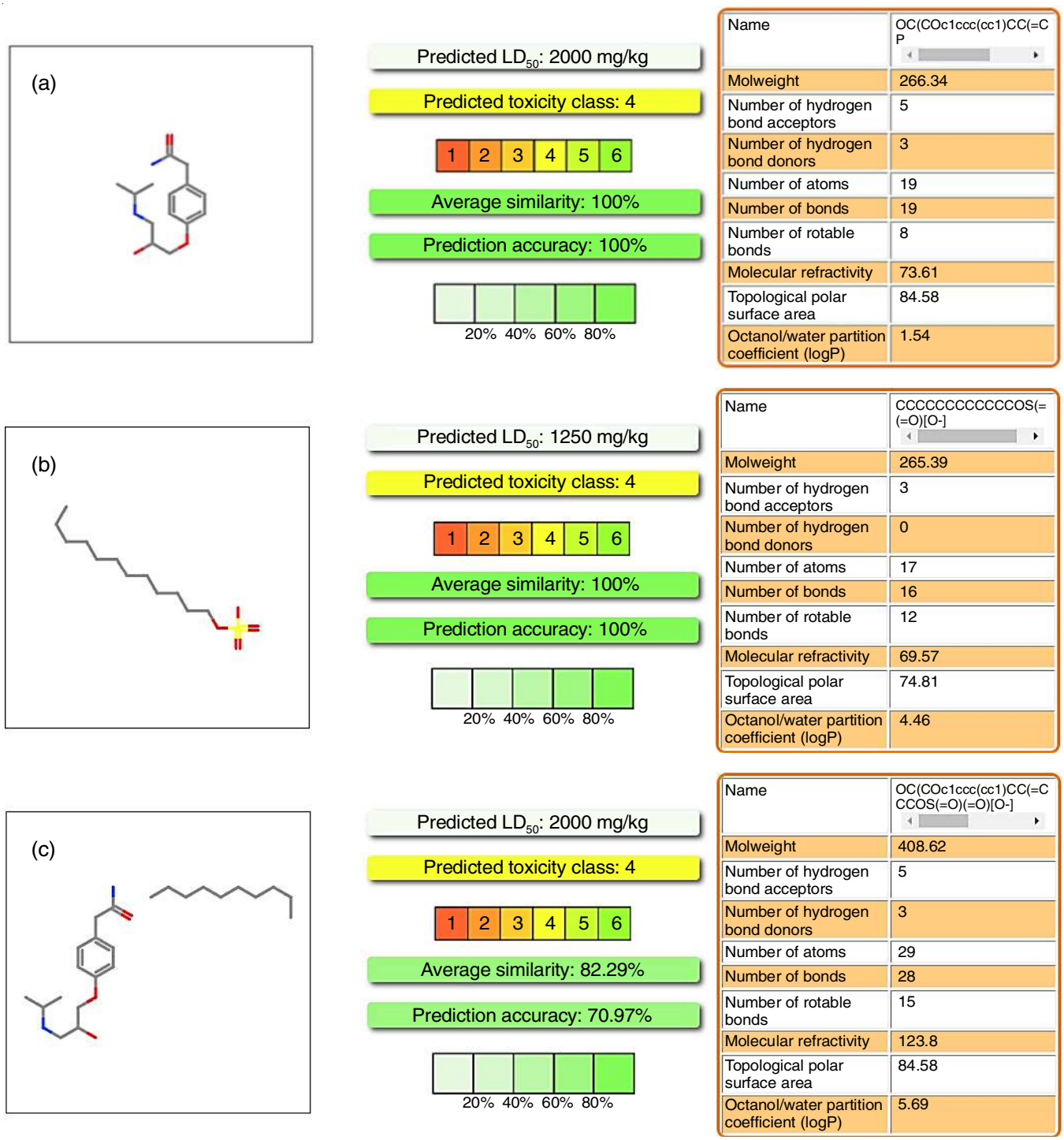

Fig. 6. Toxicity behaviour of (a) atenolol and (b) SDS (c) complex

This phenomenon can be attributed to the influence exerted by differently charged surfactant molecules and water molecules in the surroundings. As a result, there is an increase in pressure, which makes the solution more resistant to being compressed. The decrease in adiabatic compressibility as the mole fraction of CTAB rises, along with the increasing concentration of atenolol, indicates the strong interactions between solute-solvent and solute-solute, driven by the presence of CTAB and atenolol [42-44]. Acoustic impedance defined as the ratio of effective pressure applied by sound to the particle's velocity, provides significant insights into the complexity of molecular interactions within the system. The increasing values suggested the enhancement of these interactions, indicating an increased tendency for association and affinity between the two surfactants in the solution. The observed increase in the pressure-to-sound-velocity ratio indicates a correlational character of interaction [45,46].

The decrease in intermolecular free length clearly signifies a higher degree of association among the solute particles within the solution. This decrease in the intermolecular free length

TABLE-10
VARIATION OF ADIABATIC COMPRESSIBILITY, ACOUSTIC IMPEDANCE, INTERMOLECULAR FREE LENGTH AND VISCOUS RELAXATION TIME FOR SOLUTIONS IN THE ABSENCE AND PRESENCE OF ATENOLOL

Mole fraction ratio of SDS:CTAB solution	Pure surfactant solution		Surfactant solution with 1.5 mM drug		Surfactant solution with 7.5 mM drug	
	298 K	308 K	298 K	308 K	298 K	308 K
Adiabatic compressibility × 10^{-11} (pascal^{-1})						
A	44.2269	44.4139	44.1762	44.2691	43.8945	44.0672
B	43.8252	44.1281	43.7465	43.9742	43.5231	43.7121
C	43.6637	43.9176	43.6067	43.8034	43.3357	43.5879
D	43.5299	43.8132	43.4698	43.6956	43.2301	43.4081
E	43.4133	43.6886	43.3295	43.5799	43.0968	43.3007
F	43.2512	43.5715	43.1926	43.4364	42.9260	43.1826
G	43.1664	43.3947	43.0688	43.3132	42.7759	43.0138
H	42.9615	43.2651	42.8483	43.0799	42.5304	42.8310
I	42.7645	43.0451	42.5889	42.8254	42.2392	42.4977
Acoustic impedance (Z) × 10^3 rayl						
A	1502.8488	1499.1581	1504.0738	1502.0382	1509.1867	1504.4473
B	1514.3821	1507.5953	1516.6732	1511.0235	1521.4605	1516.4874
C	1518.6638	1512.1621	1519.8125	1514.6435	1525.5403	1519.2154
D	1521.4809	1514.5234	1523.3994	1516.8097	1527.9535	1522.7935
E	1524.1717	1517.1678	1527.3488	1519.4459	1530.8898	1525.3969
F	1527.4973	1520.0394	1529.1405	1522.6772	1534.5065	1528.3393
G	1529.5415	1524.2285	1531.5910	1525.8705	1537.7237	1532.3661
H	1534.1547	1527.5228	1536.5521	1531.0289	1543.0402	1536.4727
I	1538.6414	1531.9152	1542.1731	1536.1404	1549.5342	1543.2053
Intermolecular free length (L_f) × 10^{-12} m						
A	41.3632	42.1777	41.3395	42.1088	41.2075	42.0127
B	41.1749	42.0417	41.1380	41.9683	41.0328	41.8431
C	41.0990	41.9413	41.0722	41.8867	40.9443	41.7836
D	41.0360	41.8915	41.0076	41.8352	40.8944	41.6973
E	40.9810	41.8318	40.9414	41.7797	40.8314	41.6457
F	40.9044	41.7757	40.8767	41.7109	40.7503	41.5889
G	40.8643	41.6904	40.8181	41.6965	40.6790	41.5075
H	40.7672	41.6285	40.7134	41.5394	40.5621	41.4292
I	40.6737	41.5225	40.5900	41.4610	40.4230	41.2577
Viscous relaxation time × 10^{-13} sec						
A	5.4830	5.4993	5.5474	5.5910	5.5523	5.5290
B	5.5845	5.5790	5.6315	5.6093	5.6925	5.6447
C	5.5963	5.5916	5.6480	5.6207	5.9128	5.9356
D	5.6018	5.6051	5.6618	5.6464	6.0220	6.0188
E	5.6111	5.6253	5.6717	5.6715	6.1685	6.1083
F	5.6490	5.6310	5.6889	5.6828	6.3758	6.4312
G	5.6684	5.6520	5.7207	5.6938	6.5091	6.5655
H	5.7142	5.6821	5.7702	5.7221	6.7520	6.6518
I	6.2774	6.2242	6.3468	6.2813	6.8510	6.8399

enhanced the interactions between the molecules results in the compactness. The increase in relaxation time in conjunction with the reduction in intermolecular free length indicates a decreasing gap between solute molecules, which ultimately explains that the interactions are of an associative nature.

Conclusion

This study indicates that the critical micelle concentration (CMC) reveals sodium dodecyl sulphate (SDS, anionic surfactant) shows delayed micellization when atenolol is present as compared to cetyltrimethylammonium bromide (CTAB, cationic surfactant). The experimental findings and acoustic data indicate a preference for solute-solute interactions in aqueous solutions. The experimental confirmation of anticipated binding interactions, along with additional conformations, was facilitated by elucidating the acoustic parameters. This study demonstrates both theoretically and computationally through molecular docking and ADMET analysis and experimentally through ultrasonic and rheological studies, that the existence of molecular attraction between atenolol and the anionic surfactant SDS (sodium dodecyl sulfate) *via* hydrogen bonds and ion-ion dipole interactions. This comprehensive approach provides valuable insights into the nature of interactions between atenolol and SDS, paving the way for potential applications in various fields like control drug delivery, drug elimination, *etc*.

ACKNOWLEDGEMENTS

The authors express their sincere gratitude to the Head of the Department of Chemistry, University of Lucknow, Lucknow, India, for generously providing laboratory facilities essential

for conducting the experiments. Special acknowledgement is also extended to grant access to UV-Vis, Avance 300 NMR and FT-IR spectrometers, which were indispensable for the successful execution of this research.

CONFLICT OF INTEREST

The authors declare that there is no conflict of interests regarding the publication of this article.

REFERENCES

1. R.E. Baker, A.S. Mahmud, I.F. Miller, M. Rajeev, F. Rasambainarivo, B.L. Rice, S. Takahashi, A.J. Tatem, C.E. Wagner, L.-F. Wang, A. Wesolowski and C.J.E. Metcalf, *Nat. Rev. Microbiol.*, **20**, 193 (2022); https://doi.org/10.1038/s41579-021-00639-z
2. C. Andersson and R.S. Vasan, *Nat. Rev. Cardiol.*, **15**, 230 (2018); https://doi.org/10.1038/nrcardio.2017.154
3. D.R. Jacobs Jr., J.G. Woo, A.R. Sinaiko, S.R. Daniels, J. Ikonen, M. Juonala, N. Kartiosuo, T. Lehtimäki, C.G. Magnussen, J.S.A. Viikari, N. Zhang, L.A. Bazzano, T.L. Burns, R.J. Prineas, J. Steinberger, E.M. Urbina, A.J. Venn, O.T. Raitakari and T. Dwyer, *N. Engl. J. Med.*, **386**, 1877 (2022); https://doi.org/10.1056/NEJMoa2109191
4. S.P. Moulik, A.K. Rakshit and B. Naskar, *J. Surf. Deterg.*, **27**, 895 (2024); https://doi.org/10.1002/jsde.12757
5. L.M. Moreira and J.P. Lyonb, *Pubvet*, **16**, 1 (2022); https://doi.org/10.31533/pubvet.v16n04a1083.1-6
6. A. Casandra, R.-Y. Tsay, B.A. Noskov, L. Liggieri and S.-Y. Lin, *J. Taiwan Inst. Chem. Eng.*, **92**, 2 (2018); https://doi.org/10.1016/j.jtice.2018.01.042
7. S. Chakraborty, A. Chakraborty and S.K. Saha, *RSC Adv.*, **4**, 32579 (2014); https://doi.org/10.1039/C4RA03937H
8. B. Tah, P. Pal, M. Mahato and G.B. Talapatra, *J. Phys. Chem. B*, **115**, 8493 (2011); https://doi.org/10.1021/jp202578s
9. G.-G. Ying, *Environ. Int.*, **32**, 417 (2006); https://doi.org/10.1016/j.envint.2005.07.004
10. A. Mukhija and N. Kishore, *J. Mol. Liq.*, **265**, 1 (2018); https://doi.org/10.1016/j.molliq.2018.05.107
11. B.B. Herlofson and P. Barkvoll, *Acta Odontol. Scand.*, **54**, 150 (1996); https://doi.org/10.3109/00016359609003515
12. J.B. Dressman, G.L. Amidon, C. Reppas and V.P. Shah, *Pharm. Res.*, **15**, 11 (1998); https://doi.org/10.1023/A:1011984216775
13. S.M. Shaban, J. Kang and D.-H. Kim, *Composites Commun.*, **22**, 100537 (2020); https://doi.org/10.1016/j.coco.2020.100537
14. N. Yekeen, M.A. Manan, A.K. Idris and A.M. Samin, *J. Petrol. Sci. Eng.*, **149**, 612 (2017); https://doi.org/10.1016/j.petrol.2016.11.018
15. C. Vakh and S. Koronkiewicz, *Trends Analyt. Chem.*, **165**, 117143 (2023); https://doi.org/10.1016/j.trac.2023.117143
16. C. Healy, M. Paterson, S. JoystonBechal, D. Williams and M. Thornhill, *Oral Dis.*, **5**, 39 (1999); https://doi.org/10.1111/j.1601-0825.1999.tb00062.x
17. B.S. Gupta, C.-R. Shen and M.-J. Lee, *Colloids Surf. A Physicochem. Eng. Asp.*, **529**, 64 (2017); https://doi.org/10.1016/j.colsurfa.2017.05.066
18. Y. Fan, Y. Liu, J. Xi and R. Guo, *J. Colloid Interface Sci.*, **360**, 148 (2011); https://doi.org/10.1016/j.jcis.2011.04.009
19. L.Y. Zakharova et al., *Organic Materials as Smart Nanocarriers for Drug Delivery*; Elsevier, 2018; pp 601–618; https://doi.org/10.1016/B978-0-12-813663-8.00014-2
20. C. Zhang, F. Cui, G. Zeng, M. Jiang, Z. Yang, Z. Yu, M. Zhu and L. Shen, *Sci. Total Environ.*, **518–519**, 352 (2015); https://doi.org/10.1016/j.scitotenv.2015.03.007
21. S.E. Jørgensen and B. Halling-Sørensen, *Chemosphere*, **40**, 691 (2000); https://doi.org/10.1016/S0045-6535(99)00438-5
22. H.A. Navare, R.F. Frye, R.M. Cooper-DeHoff, J.J. Shuster, K. Hall, S.O.F. Schmidt, S.T. Turner and J.A. Johnson, *Pharmacotherapy*, **30**, 872 (2010); https://doi.org/10.1592/phco.30.9.872
23. H. Al-Hamidi, A.A. Edwards, M.A. Mohammad and A. Nokhodchi, *Colloids Surf. B Biointerfaces*, **76**, 170 (2010); https://doi.org/10.1016/j.colsurfb.2009.10.030
24. S. Gupta, R. Kesarla and A. Omri, *ISRN Pharm.*, **2013**, 848043 (2013); https://doi.org/10.1155/2013/848043
25. S. Chauhan, M.S. Chauhan, D. Kaushal, V.K. Syal and J. Jyoti, *J. Solution Chem.*, **39**, 622 (2010); https://doi.org/10.1007/s10953-010-9534-9
26. J. Ramyasree, A.A. Hindustan, H. Chinthaguinjala, T. Reshma, H.V.C. Venkata and K.Y. Bharath, *Int. J. Pharma Bio Sci.*, **10**, (2020); https://doi.org/10.22376/ijpbs/lpr.2020.10.5.P11-16
27. S. Sarkar, G. Chakraborty and H. Pal, *Colloids Surf. B Biointerfaces*, **237**, 113839 (2024); https://doi.org/10.1016/j.colsurfb.2024.113839
28. G. Pifferi, P. Santoro and M. Pedrani, *Farmaco*, **54**, 1 (1999); https://doi.org/10.1016/S0014-827X(98)00101-3
29. A. Delmonte, F.F. Visentini, J.L. Fernández, L.G. Santiago and A.A. Perez, *Colloids Surf. B Biointerfaces*, **235**, 113783 (2024); https://doi.org/10.1016/j.colsurfb.2024.113783
30. A. Singh, K.R. Ansari, I.H. Ali, N. Raj Sharma, A. Bansal, A.K. Alanazi, M. Younas, A.H. Alamri, Y. Lin and A. Noureldeen, *J. Mol. Liq.*, **391**, 123305 (2023); https://doi.org/10.1016/j.molliq.2023.123305
31. M. Rahman, A. Hussain, M.S. Hussain, M.A. Mirza and Z. Iqbal, *Drug Dev. Ind. Pharm.*, **39**, 1 (2013); https://doi.org/10.3109/03639045.2012.660949
32. C. Das and B. Das, *J. Chem. Eng. Data*, **54**, 559 (2009); https://doi.org/10.1021/je8005024
33. J. Fan, A. Fu and L. Zhang, *Quant. Biol.*, **7**, 83 (2019); https://doi.org/10.1007/s40484-019-0172-y
34. L.H. Blanco and E.F. Vargas, *Instrum. Sci. Technol.*, **32**, 13 (2004); https://doi.org/10.1081/CI-120027343
35. I. Saxena, R.N. Pathak, V. Kumar and R. Devi, *Int. J. Appl. Res.*, **1**, 562 (2018); https://doi.org/10.13140/RG.2.2.35801.83044
36. M.A. ZielinskaPisklak, D.M. Pisklak and I. Wawer, *Magn. Reson. Chem.*, **49**, 284 (2011); https://doi.org/10.1002/mrc.2742
37. M. Dzida, M. Chorazewski, M. Geppert-Rybczynska, E. Zorebski, M. Zorebski, M. Zarska and B. Czech, *J. Chem. Eng. Data*, **58**, 1571 (2013); https://doi.org/10.1021/je301192s
38. D.F. Veber, S.R. Johnson, H.-Y. Cheng, B.R. Smith, K.W. Ward and K.D. Kopple, *J. Med. Chem.*, **45**, 2615 (2002); https://doi.org/10.1021/jm020017n
39. A.K. Ghose, V.N. Viswanadhan and J.J. Wendoloski, *J. Comb. Chem.*, **1**, 55 (1999); https://doi.org/10.1021/cc9800071
40. J.S. Delaney, *J. Chem. Inf. Comput. Sci.*, **44**, 1000 (2004); https://doi.org/10.1021/ci034243x
41. B. Iskandar, H.-C. Mei, T.-W. Liu, H.-M. Lin and C.-K. Lee, *Colloids Surf. B Biointerfaces*, **234**, 113692 (2024); https://doi.org/10.1016/j.colsurfb.2023.113692
42. R.J. Fort and W.R. Moore, *Trans. Faraday Soc.*, **61**, 2102 (1965); https://doi.org/10.1039/tf9656102102
43. W. Marczak, *J. Chem. Eng. Data*, **41**, 1462 (1996); https://doi.org/10.1021/je960185i
44. S. Hoche, M.A. Hussein and T. Becker, *Ultrasonics*, **57**, 65 (2015); https://doi.org/10.1016/j.ultras.2014.10.017
45. K. Ito, K. Yoshida, H. Maruyama, J. Mamou and T. Yamaguchi, *Ultrasound Med. Biol.*, **43**, 700 (2017); https://doi.org/10.1016/j.ultrasmedbio.2016.11.011
46. K. Saravanakumar, R. Baskaran and T.R. Kubendran, *Russ. J. Phys. Chem. A. Focus Chem.*, **86**, 1947 (2012); https://doi.org/10.1134/S0036024412130195